BUTTERWORTH HEINEMANN

Polymer Vol. 36 No. 6, pp. 1261–1268, 1995

0032-3861/95/$10.00+0.00

Synthesis and liquid-crystalline properties of polyacrylates containing prochiral sulfide substituents

Michele Laus and Annino S. Angeloni
Dipartimento di Chimica Industriale e dei Materiali, Università di Bologna, 40136 Bologna, Italy

and Giancarlo Galli and Emo Chiellini*
Dipartimento di Chimica e Chimica Industriale, Università di Pisa, 56126 Pisa, Italy

and Oriano Francescangeli and Bin Yang
Dipartimento di Scienze dei Materiali e della Terra, Università di Ancona, 60131 Ancona, Italy
(Received 28 March 1994; revised 5 September 1994)

The synthesis and thermal behaviour of a new series of side-chain liquid-crystalline polyacrylates **1a–h** containing prochiral alkyl sulfide substituents with a variable number n of carbon atoms are described. No liquid-crystalline behaviour was exhibited in the melt by the relevant monomers and intermediate compounds. In contrast, all polymers displayed thermotropic properties. The lower homologues **1a–f** ($n \leqslant 6$) displayed smectic B1 and smectic A1 mesophases, while the higher homologue **1h** ($n = 10$) formed a bilayer, partly interdigitated smectic C mesophase. A special position was held by **1g** with a sulfide substituent of intermediate length ($n = 8$), for which monolayer and bilayer smectic mesophases coexisted over a wide temperature range.

(Keywords: liquid-crystalline polymers; monolayer smectic mesophase; mesophase coexistence)

INTRODUCTION

The design and synthesis of chiral thermotropic side-chain liquid-crystalline polymers are currently the focus of intense research[1,2]. The ability of these polymers to generate chiral nematic (cholesteric) and chiral smectic supramolecular assemblies endowed with a macroscopic twist can result in the availability of new materials with promising optical and electro-optical properties for various potential high-tech applications[3–5].

The primary routes to the synthesis of chiral side-chain liquid-crystalline polymers are the chain polymerization of mesogenic monomers containing chiral moieties with preferential chirality and the copolymerization of a mesogenic comonomer with a chiral one, mesogenic or not. Additionally, polymer-analogue reactions are extensively adopted for the synthesis of chiral liquid-crystalline polymers, for instance by grafting chiral mesogenic olefins or vinyl ethers onto poly(hydrogensiloxane) parent polymers[5]. Very recently, a complementary approach has been reported[6–8] consisting in the enantioselective modification of prochiral polymeric substrates. This synthetic strategy, even though often limited by the unpredictable and low optical yields, is particularly attractive for its apparent simplicity and the opportunities it offers to realize molecular architectures otherwise unfeasible by more conventional synthetic procedures. However, the asymmetric modification reaction should be highly selective from chemical and stereochemical standpoints and, in addition, should not induce any undesired side reaction of the polymer structure. Following this synthetic approach, we described a convenient route to the preparation of chiral liquid-crystalline main-chain polymers by the enantioselective oxidation of the corresponding parent polymers containing prochiral sulfide groups in the main chain[6,7]. Very recently, we extended[8] this asymmetric modification to two specifically designed side-chain polymers **1b** and **1d** of a new class

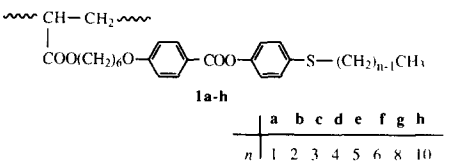

1a-h

	a	b	c	d	e	f	g	h
n	1	2	3	4	5	6	8	10

Prochiral sulfide groups, such as those present in the repeat units of **1a–h**, can undergo an asymmetric oxidation leading to chiral sulfoxides with moderate to high enantiomeric excess[9,10]. This enantioselective modification will introduce a strong dipole moment directly at the chiral moiety and perpendicular to the long molecular axis of the mesogenic unit. In turn, these structural features may be expected to be conducive to

*To whom correspondence should be addressed

chiral smectic C* polymers with ferroelectric and non-linear optical properties[5].

Following this line, we extended our investigation to several new homologues of the polyacrylate series **1a–h**. They contain a mesogenic unit linked to the polymer backbone by a hexamethylene spacer and substituted in the 4-position by an alkyl sulfide substituent of variable length ($n = 1$–$6, 8, 10$). In the present paper we describe their synthesis, structure and liquid-crystalline properties. The enantioselective oxidation leading to the corresponding chiral polymers **2a–h** will be described in a forthcoming paper.

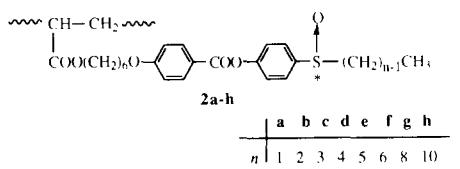

Polyacrylates **1a–h** displayed a mesomorfic behaviour that depended very much upon the length of the alkyl sulfide tail. Unusually for side-chain polymers[11–13], **1g** showed different smectic mesophases coexisting in equilibrium over an extremely wide temperature range (up to 40 K)[14]. A combination of critical molecular and structural factors was invoked to interpret this peculiar phase behaviour. In this respect, the present study of the liquid-crystalline properties of the class **1a–h** provides further substantiation to the above interpretation.

EXPERIMENTAL

Materials

4-(Benzyloxycarbonyloxy)benzoyl chloride[15] **2** and 1-chloro-6-acryloyloxyhexane[8] **6** were prepared according to literature methods. 4-Hydroxyphenyl alkyl sulfides **3a–h** were synthesized by way of a general synthetic procedure[8]. Polymers **1a–h** were prepared by the experimental procedure used for polymer **1a**, which is reported in detail as a typical example.

4-[(4-Benzyloxycarbonyloxy)benzoyloxy]phenyl methyl sulfide ***4a***. A solution of 10.7 g (36.8 mmol) of **2** in 50 ml of anhydrous 1,2-dichloroethane was added to a solution containing 5.2 g (36.8 mmol) of **3a**, 1.5 g (37.5 mmol) of sodium hydroxide and 1.0 g of benzyltributylammonium bromide in 50 ml of water. The mixture was stirred for 15 min. The organic layer was isolated, washed with 1.0 M sodium hydroxide and then water, dried over sodium sulfate and evaporated under vacuum. The solid product was recrystallized from ethyl acetate/cyclohexane (1/1 v/v). The product had a melting point of 201°C. The yield was 65%. ^{1}H n.m.r. (δ values in $CDCl_3$): 8.1 (d, 2H); 7.5–7.1 (m, 11H); 5.3 (s, 2H); 2.8 (s, 3H).

4(4-Hydroxybenzoyloxy)phenyl methyl sulfide ***5a***. A mixture of 5.0 g (12.6 mmol) of **4a**, 20 ml of 1.0 M sodium hydroxide and 100 ml of 95% ethanol was refluxed for 30 min. The reaction mixture was cooled to room temperature, filtered and acidified with hydrochloric acid. The precipitate was filtered, washed with water and purified by recrystallization from benzene/n-hexane (1/1 v/v). The product was obtained in 92% yield and melted at 113°C. ^{1}H n.m.r. (δ values in $CDCl_3$): 8.1 (d, 2H); 7.4 (d, 2H); 7.2 (d, 2H); 6.9 (d, 2H); 5.8 (s, 1H); 2.8 (s, 3H).

4-[4-(6-Acryloyloxyhexyloxy)benzoyloxy]phenyl methyl sulfide ***7a***. A mixture of 3.2 g (16.8 mmol) of **6**, 1.6 g (6.3 mmol) of **5a**, 1.3 g (9.4 mmol) of dry potassium carbonate and 0.2 g of 2,6-di-t-butyl-4-methylphenol in 40 ml of dry dimethyl sulfoxide was heated to 120°C. After 30 min, the mixture was poured into 100 ml of 0.5 M sodium hydroxide. The crude product was washed with 2 × 50 ml of cold water and dissolved in 50 ml of chloroform. The resultant solution was dried over sodium sulfate and evaporated under vacuum. The crude product was crystallized from n-hexane. The product was obtained in 42% yield and melted at 49°C. ^{1}H n.m.r. (δ values in $CDCl_3$): 8.1 (d, 2H); 7.4 (d, 2H); 7.2 (d, 2H); 6.9 (d, 2H); 6.5–5.8 (m, 3H); 4.2 (t, 2H); 4.1 (t, 2H); 2.8 (s, 3H); 1.9–1.2 (m, 8H).

Melting temperatures, crystallization solvents and reaction yields of monomers **7a–h** and the relevant intermediates **4a–h** and **5a–h** are collected in *Table 1*.

Synthesis of polymers ***1a–h***. In a typical polymerization reaction, 1.0 g of acrylate monomer was dissolved in 5 ml of dry benzene in the presence of 5.0 mg of 2,2′-azobisisobutyronitrile (AIBN). The reaction mixture was introduced into a Pyrex glass ampoule, thoroughly freeze–thaw degassed and sealed in the ampoule under vacuum. After 48 h of reaction at 60°C, the resultant polymer was recovered by addition of 100 ml of methanol. It was then precipitated twice from chloroform solution into methanol and purified by extraction with boiling methanol in a Kumagawa extractor. The polymeric product was then dried under vacuum for 6 h.

Instrumental techniques

^{1}H n.m.r. and ^{13}C n.m.r. spectra were recorded on a Varian Gemini 200 spectrometer. Average molar masses

Table 1 Characteristics of intermediates **4a–h** and **5a–h** and acrylate monomers **7a–h**

Sample	Solvent for crystallization	Yield (%)	T_m (°C)
4a	Ethyl acetate/cyclohexane (1/1 v/v)	65	201
4b	Cyclohexane	70	77
4c	Ethanol	80	80
4d	Ethanol	59	80
4e	Cyclohexane	48	79
4f	Cyclohexane	80	90
4g	Ethanol	60	94
4h	Cyclohexane	77	103
5a	Benzene/n-hexane (1/1 v/v)	92	113
5b	Benzene	90	167
5c	Benzene/n-hexane (1/1 v/v)	72	148
5d	Benzene/n-hexane (1/1 v/v)	60	80
5e	Benzene/n-hexane (1/1 v/v)	66	120
5f	Benzene/n-hexane (1/1 v/v)	73	135
5g	Benzene	60	121
5h	Cyclohexane	70	125
7a	n-Hexane	42	49
7b	Methanol	50	77
7c	Methanol	61	64
7d	Methanol	52	64
7e	Methanol	50	70
7f	Methanol	48	60
7g	Methanol	50	61
7h	Methanol	36	70

were determined by size exclusion chromatography (s.e.c.) of chloroform solutions with a Waters 590 chromatograph equipped with a Shodex KF-804 column. Polystyrene standard samples were used for the universal calibration method[16]. Differential scanning calorimetry (d.s.c.) analyses were carried out under a dry nitrogen flow with a Perkin–Elmer DSC-7 apparatus. The temperature scale was calibrated against the melting temperature of indium. For the determination of the transition enthalpy, indium was used as a standard material. The transition temperatures were taken from the d.s.c. traces of samples annealed by cooling from the isotropic melt as corresponding to the maxima and the onset points of the enthalpic peaks for polymers and low-molar-mass samples, respectively, at a heating rate of $10\,K\,min^{-1}$. Optical microscopy observations were performed on polymer films sandwiched between glass slides. A Reichert Polyvar microscope equipped with a programmable Mettler FP52 heating stage operating at a scanning rate of $10\,K\,min^{-1}$ was used.

Oriented smectic phases were produced by drawing fibres out of the mesophase at a temperature 20 K lower than the smectic–isotropic transition temperature with a pair of tweezers and cooling them in air at room temperature. Accordingly, the average chain axis of the polymer corresponds to the fibre axis. X-Ray measurements were performed by using a Rigaku Denki RV300 rotating anode generator equipped with a flat pinhole camera. Ni-filtered $CuK_{\alpha 1}$ ($\lambda = 1.54$ Å) radiation was used.

RESULTS AND DISCUSSION

Polymers **1a–h** were prepared by the synthetic procedure represented in *Scheme 1*. 4-(4-Hydroxybenzoyloxy)phenyl alkyl sulfides **5a–h** were prepared by reacting the sodium salts of the corresponding 4-hydroxyphenyl alkyl sulfides **3a–h** with 4-(benzyloxycarbonyloxy)benzoyl chloride **2** using a catalytic amount of benzyltributylammonium bromide as the phase transfer agent and removing the benzyloxycarbonyl protecting group by alkaline hydrolysis of **4a–h**. 4-[4-(6-Acryloyloxyhexyloxy)benzoyloxy]-phenyl alkyl sulfides **7a–h** were obtained by reacting phenols **5a–h** with 1-chloro-6-acryloyloxyhexane **6** in the presence of potassium carbonate and a small amount of free radical inhibitor in dry dimethyl sulfoxide.

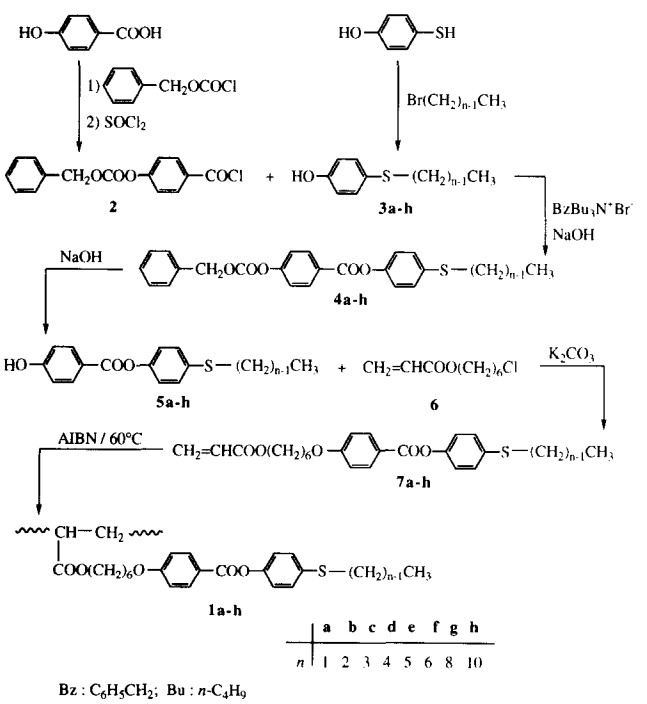

Scheme 1 Synthetic route for the preparation of polyacrylates **1a–h**

Polymers **1a–h** were obtained by free radical initiation (AIBN) at 60°C with polymerization yields in the range 85–90%. Purification of the polymers was accomplished by reprecipitation from chloroform solution into methanol and continuous extraction with boiling methanol. The molar mass characteristics of the polyacrylates were determined by s.e.c. and are listed in *Table 2*. The number average molar mass (M_n) ranged from 42 000 to 195 000 g mol^{-1} with the first polydispersity index (M_w/M_n) between 1.9 and 3.4. Therefore, M_n was substantially greater than the limiting value of 10 000 g mol^{-1}, above which it is usually claimed[17,18] that the liquid-crystalline phase transition parameters become independent of the molar mass. The molar mass distribution of polymers **1a–h** was moderately wide and, according to very recent findings[19,20], relatively broad biphasic regions may occur.

The phase transition temperatures and relevant thermodynamic parameters were determined by d.s.c. measurements. The liquid-crystalline behaviour was qualitatively confirmed by polarizing microscopy, as specific optical textures of the mesophases were not observed. The nature of the mesophases of the polymers was identified by X-ray diffraction on unoriented and oriented specimens. No mesophases were observed for monomers **7a–h** and the intermediate compounds **4a–h** and **5a–h**. In contrast, all polymers **1a–h** exhibited liquid-crystalline behaviour in the melt. The phase transition thermodynamic parameters and relevant phase assignments are summarized in *Table 2*. Polymers **1a–f** had a qualitatively similar thermal behaviour. In the d.s.c. heating curves (*Figures 1a–f*), two endothermic peaks were connected to a transition between smectic mesophases and a smectic–isotropic transition. The glass transition was also detected as a weak step increase in heat capacity (see, for instance, *Figures 1b* and *1g*). All these transitions were reversible on cooling (*Figures 2a–f*). An additional intermediate endotherm of low intensity ($\Delta H = 2.5$ kJ mol^{-1}) was seen in the heating curve of **1h** only (*Figure 1h*), owing to the melting of minor crystalline regions grown under non-

Table 2 Physicochemical properties of polymers **1a–h**

Sample	M_n[a] (g mol^{-1})	M_w/M_n[a]	Phase transition temperatures (K) (entropies in parentheses (J mol^{-1} K^{-1}))[b]
1a	65 000	2.8	g305S_{B1}308(1.0)S_{A1}387(7.7)I
1b	66 000	2.6	g301S_{B1}310(3.2)S_{A1}384(9.2)I
1c	51 000	2.2	g296S_{B1}308(4.6)S_{A1}363(10.3)I
1d	81 000	3.4	g295S_{B1}303(4.2)S_{A1}362(11.1)I
1e	119 000	3.1	g311S_{B1}319(7.1)S_{A1}365(12.8)I
1f	42 000	2.0	g315S_{B1}321(7.0)S_{A1}362(14.6)I
1g	62 000	1.9	g299S_{B1} + S_{Bd}314(2.45)S_{A1} + S_{Ad}352(6.5)S_{Ad}365(11.1)I
1h	195 000	3.2	g318S_{Cd}394(21.9)I

[a] By s.e.c. in chloroform at 30 C

[b] g, frozen glassy mesophase; S_{B1}, monolayer smectic B; S_{Bd}, interdigitated bilayer smectic B; S_{A1}, monolayer smectic A; S_{Ad}, interdigitated bilayer smectic A; S_{Cd}, interdigitated bilayer smectic C; I, isotropic (by d.s.c.)

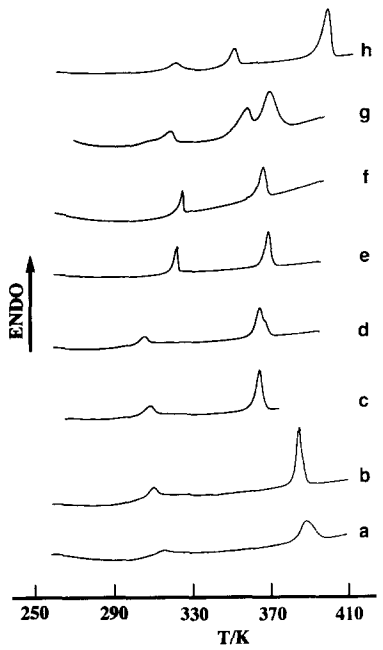

Figure 1 D.s.c. second-heating scans (10 K min^{-1}) of polyacrylates **1a** (a), **1b** (b), **1c** (c) **1d** (d), **1e** (e), **1f** (f), **1g** (g) and **1h** (h)

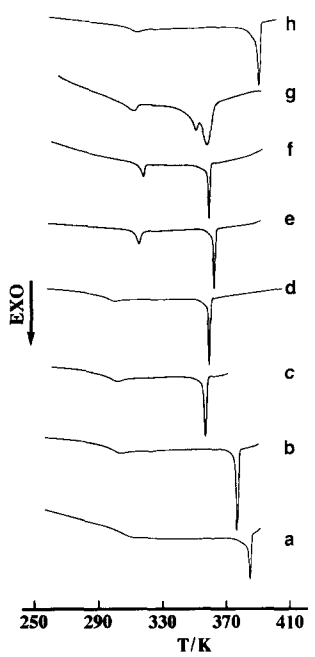

Figure 2 D.s.c. first-cooling scans (10 K min^{-1}) of polyacrylates **1a** (a), **1b** (b), **1c** (c), **1d** (d), **1e** (e), **1f** (f), **1g** (g) and **1h** (h)

isothermal conditions during the scan. Crystallization was not detected on cooling (*Figure 2h*), nor was any crystallinity detected by X-ray diffraction (see below). For each polymer, optical microscopy observations demonstrated that the high-temperature endotherm corresponded to a smectic–isotropic transition.

The X-ray diagrams of powder samples of **1a–f** are very similar. Typical X-ray diagrams at different temperatures from room temperature up to the isotropization point for **1e** are shown in *Figure 3*. At room temperature, they each consist of one low-angle peak corresponding to a periodicity d in Å of 25.6 (**1a**), 26.5 (**1b**), 27.4 (**1c**), 28.4 (**1d**), 29.3 (**1e**) and 30.2 (**1f**), and one rather sharp wide-angle peak from a periodicity $D \approx 4.4$ Å (*Figure 3a*). This is consistent with the presence of an ordered smectic structure with a layer spacing of d and an intermolecular distance between side-chain mesogens of D. The wide-angle signals became very diffuse above the temperature relevant to the lower-temperature d.s.c. endothermic transition (*Figure 3c*). The broadening of the wide-angle peak indicates a loss of the lateral correlation among the molecular segments within the smectic layers at the transition from an ordered smectic mesophase to a disordered one. The resulting X-ray diffraction diagrams, consisting of one sharp low-angle peak and one diffuse wide-angle halo, remained unchanged until the temperature of the higher-temperature d.s.c. transition was reached. Above this temperature, the low-angle signal vanished, in keeping with the occurrence of a transition to the isotropic melt (*Figure 3e*). In all the above samples, the smectic interlayer spacing d was practically constant from room temperature up to the isotropization point, as illustrated for **1a** and **1e** in *Figure 4*. The values of d for polymers **1a–f** are in close agreement with the lengths L of their respective side chains ($L = 25.0$, 26.3, 27.5, 28.8,

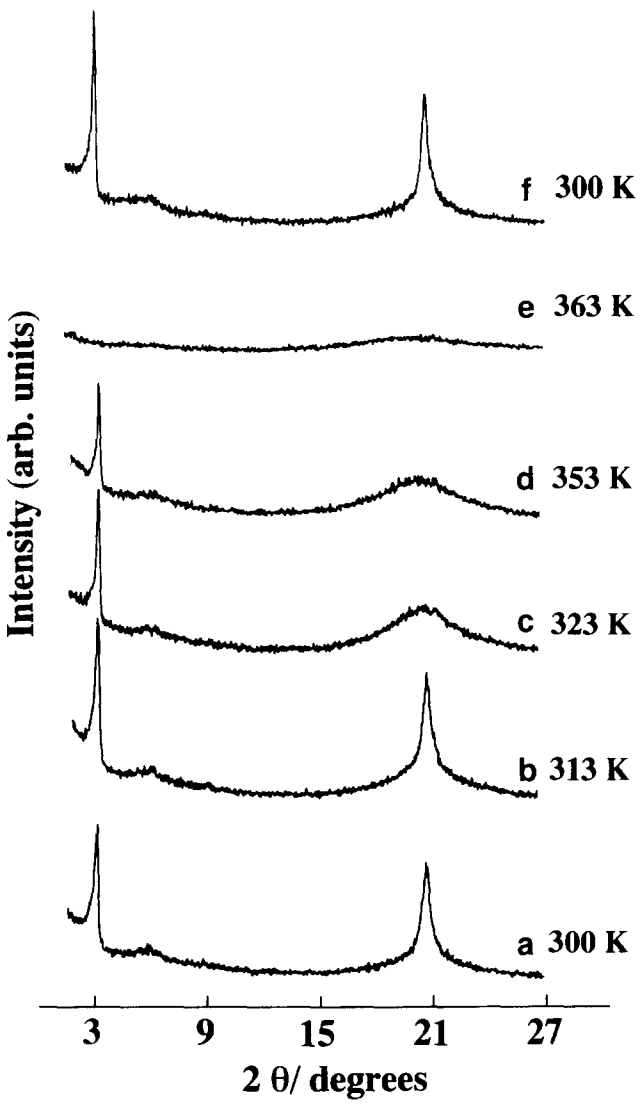

Figure 3 X-Ray diffraction diagrams of polymer **1e** at different temperatures. The bottom and top curves at 300 K refer to the as-prepared and annealed samples, respectively

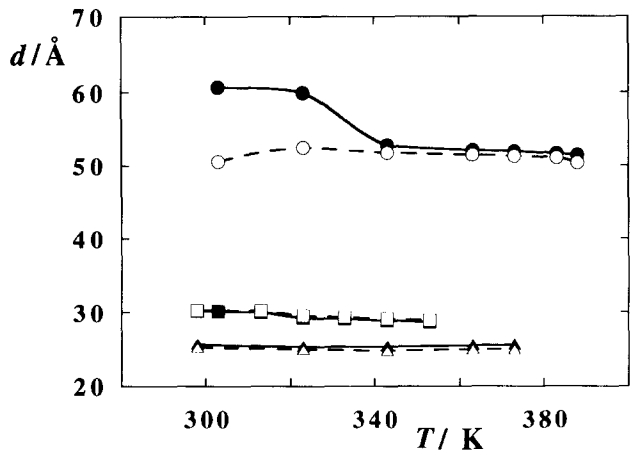

Figure 4 Changes in the interlayer spacings d for polymers **1a** (▲, △), **1e** (■, □) and **1h** (●, ○) as a function of temperature. Full and open symbols refer to the second heating (first heating for **1h**) and cooling cycles, respectively

30.1 and 31.3 Å) as calculated from standard bond lengths and angles under the assumption of an all-*trans* conformation of the methylene segments in the side chains. Thus, the smectic phase had a monolayer structure.

The X-ray diffraction diagram of polymer **1h** at room temperature consists of two low-angle signals with $d = 60.7$ and 30.3 Å, corresponding to two orders of reflection, and a diffuse wide-angle halo at $D \approx 4.4$ Å (*Figure 5a*). On heating the sample above the glass transition, the low-angle signals became better resolved and the spectrum was made up of three sharp low-angle signals with $d = 54.8$, 27.4 and 18.3 Å (at 343 K), corresponding to three orders of reflection, and a diffuse wide-angle halo at $D \approx 4.4$ Å (*Figure 5b*). This X-ray diffraction pattern is characteristic of the disordered smectic A or C phase. The interlayer spacing d of as-prepared **1h** decreased on the first heating from room temperature to 330–340 K, but it was essentially constant with varying temperature in annealed samples (*Figure 4*). As the smectic interlayer spacing of **1h** was much longer than the length L of the repeat unit in the fully extended conformation ($L = 37.0$ Å), as estimated from Dreiding stereomodels, some form of bilayer arrangement of the side chains in the smectic mesophase was involved.

To gain a better understanding of the structure of these smectic mesophases, X-ray diffraction measurements on polymer fibres were also performed. Oriented smectic phases were produced by drawing fibres out of the mesophase at a temperature 20 K lower than the smectic–isotropic transition temperature and cooling them in air at room temperature. The X-ray diagrams of the oriented samples **1a–f** are very similar to each other. *Figure 6* illustrates the X-ray fibre pattern of **1e** as a typical example of this set of polymers. The anisotropy shown in the X-ray diffraction of all the polymer samples clearly demonstrates that a high degree of molecular orientation could be achieved by drawing fibres from the mesophases. In the low-angle region, there are eight Bragg spots (only six are easily visible in *Figure 6*) corresponding to the first four orders of reflection on the smectic layers. They are aligned on the equator, thus indicating that the smectic layers are parallel to the fibre axis. The two rather sharp spots on the meridian in the wide-angle pattern demonstrate the existence of a certain

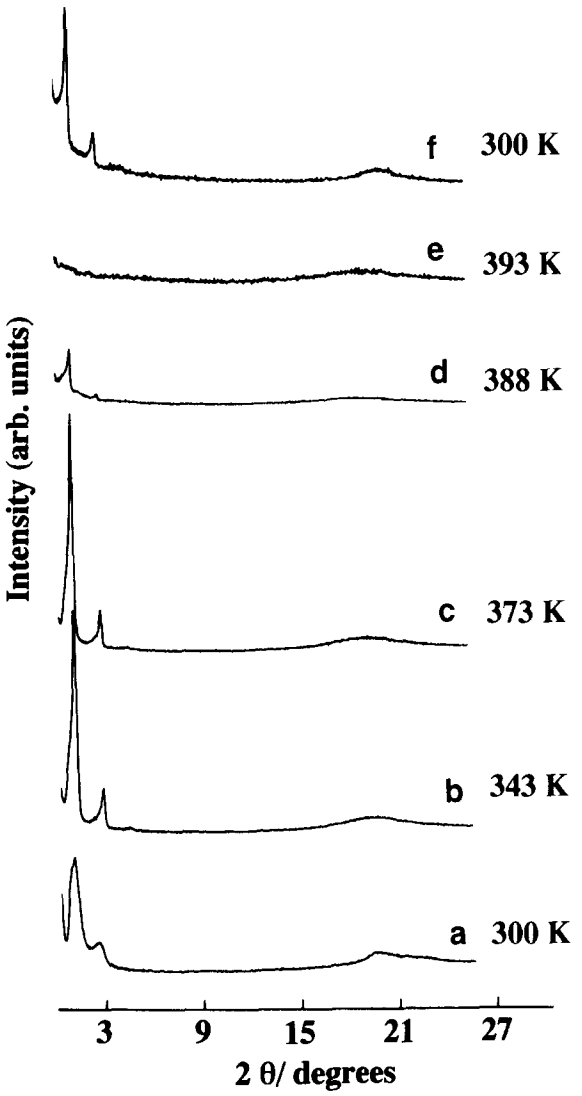

Figure 5 X-ray diffraction diagrams of polymer **1h** at different temperatures. The bottom and top curves at 300 K refer to the as-prepared and annealed samples, respectively

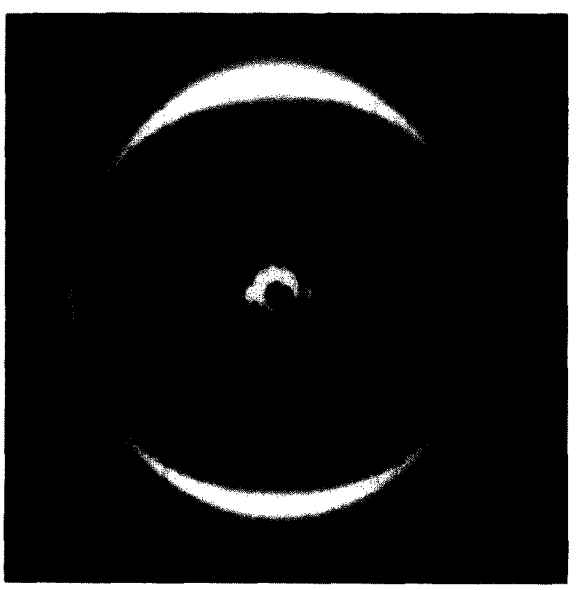

Figure 6 Fibre X-ray diffraction pattern of polymer **1e** (vertical fibre axis)

degree of order within the layers of the side-chain mesogens. In addition, the mesogenic groups are perpendicular to the smectic layers, and accordingly the higher-temperature and lower-temperature mesophases of polymers **1a–f** can be identified as S_{A1} and S_{B1}, respectively. This is in keeping with a structural model in which the polymer backbone is oriented parallel to the fibre axis. For all samples **1a–f** the structure of the lower-temperature mesophase was frozen in at room temperature. In the smectic B mesophase, the mesogenic groups packed in a hexagonal array[21] with a lattice parameter $a = 5.2$ Å.

The X-ray diffraction pattern of the oriented sample **1h** differs substantially from the patterns of **1a–f** (*Figure 7*). In the low-angle region, there are six Bragg spots corresponding to the first three orders of reflection on the smectic layers. They are aligned on the equator, thus showing that the layers are parallel to the fibre axis. In the wide-angle region, four diffuse spots are roughly equidistant from the origin and form pairs on straight lines making an angle β of about 40° with respect to the fibre axis. Therefore, the mesogenic side groups are tilted to the layer normal in a smectic C mesophase[22,23] by an angle $\beta \approx 40°$. The values of β, d and L indicate that a little overlap of the side chains should occur in an interdigitated smectic C phase (S_{Cd}).

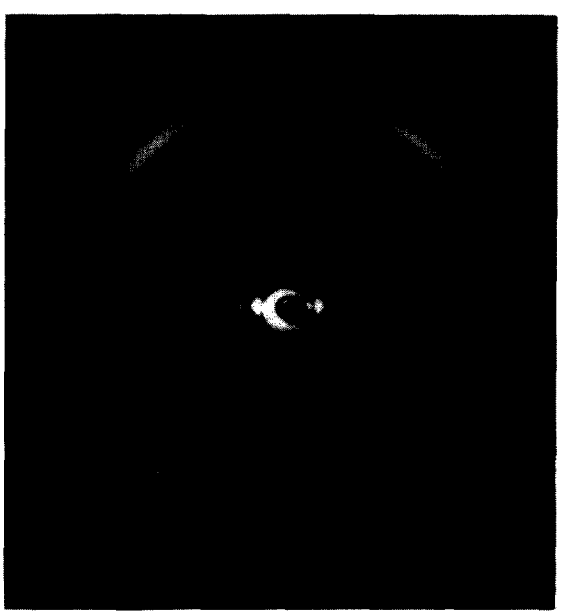

Figure 7 Fibre X-ray diffraction pattern of polymer **1h** (vertical fibre axis)

The liquid-crystalline behaviour of polymer **1g** has recently been described in some detail[14]. In the relevant d.s.c. heating curve (*Figure 1g*), the glass transition at 299 K and three endothermic transitions at 314, 352 and 365 K are detected. On cooling the sample (*Figure 2g*), all these transitions reappear with relatively small degrees of supercooling. The following mesophase sequence has been determined

$$g \xrightarrow{299K} S_{B1} + S_{Bd} \xrightarrow{314K} S_{A1} + S_{Ad} \xrightarrow{352K} S_{Ad} \xrightarrow{365K} I$$

Two smectic B (S_B) mesophases, one of which is monolayer (S_{B1}) and the other bilayer interdigitated (S_{Bd}), or alternatively S_B and smectic A (S_A) mesophases[14], coexist in the temperature range between 299 and 314 K. In addition, an interdigitated smectic A (S_{Ad}) mesophase with $d = 52.4$ Å and a monolayer smectic A (S_{A1}) mesophase with $d = 34.6$ Å coexist in the temperature range between 314 and 352 K. Above 352 K, one S_{Ad} phase with $d = 52.2$ Å occurs. The structures of the different disordered smectic mesophases of polymers **1a–h** are sketched in *Figure 8*.

The trends of the glass transition, S_{B1}–S_{A1} and isotropization temperatures of polymers **1a–f** as a function of the number n of carbon atoms in the alkyl sulfide substituent are illustrated in *Figure 9*. The glass transition temperature decreases slightly up to $n = 4$ and then rises with increasing n, probably owing to a plasticizing effect of the terminal alkyl tails which is then offset in the higher homologues, in agreement with common findings in vinyl polymers[24]. The stability of the S_{A1} mesophase decreases, whereas the stability of the S_{B1} mesophase increases with increasing n. This results in a broad persistence range of the mesophase for the lower homologues (>80 K for **1a** and **1b**), tending to narrow for the higher homologues (47 K for **1f**). The

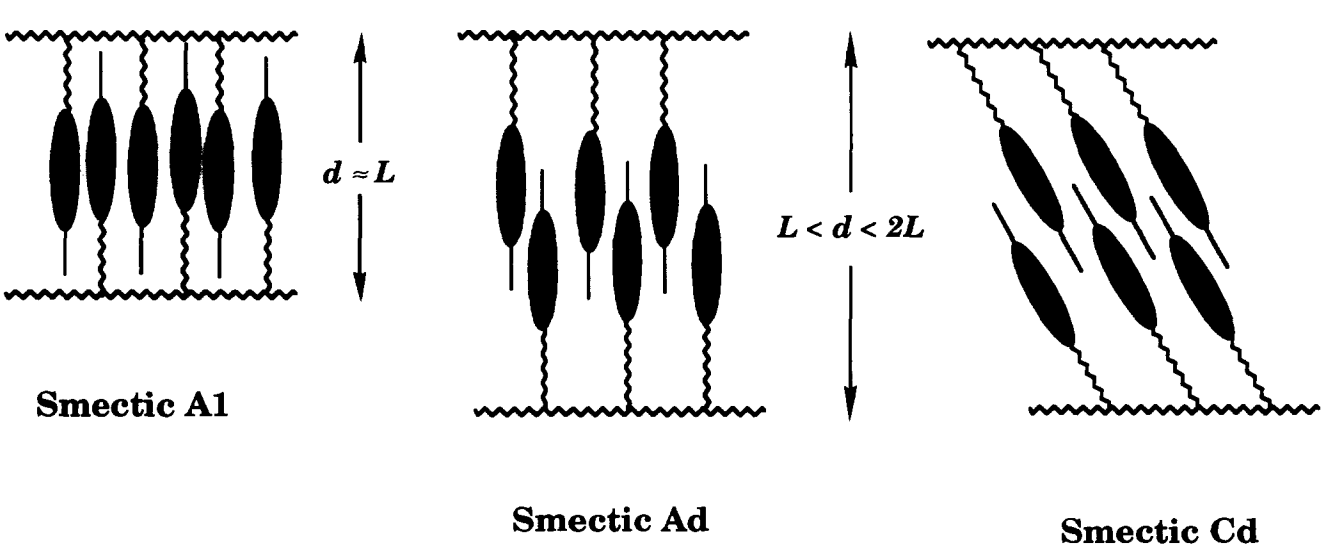

Figure 8 Schematic representation of the S_{A1}, S_{Ad} and S_{Cd} mesophases

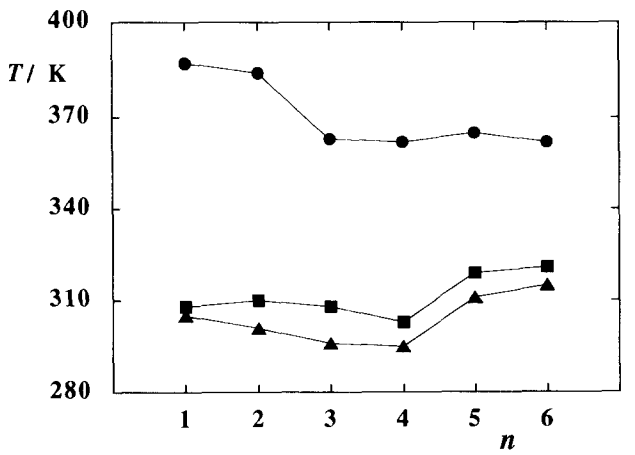

Figure 9 Phase transition temperatures for polyacrylates **1a–f** as a function of the alkyl sulfide length (n): (▲) glass transition; (■) S_{B1}–S_{A1} transition; (●) S_{A1}–isotropic transition

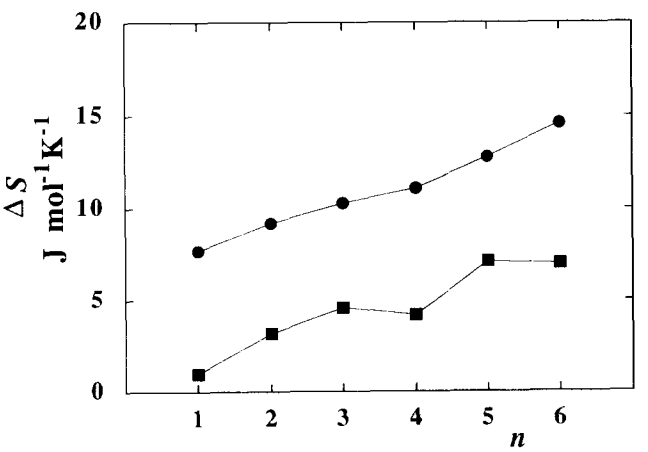

Figure 10 Phase transition entropies for polyacrylates **1a–f** as a function of the alkyl sulfide length (n): (■) S_{B1}–S_{A1} transition; (●) S_{A1}–isotropic transition

range of existence of the S_{B1} mesophase was in any case rather limited, reaching the widest value (12 K) for **1c**. *Figure 10* shows the trends of the S_{B1}–S_{A1} and isotropization entropies of polymers **1a–f** as a function of n. Both the S_{B1}–S_{A1} and S_{A1}–isotropic transition entropies increase with increasing n, thus indicating an increasing contribution of the conformational freedom to the transition entropy associated with each transition.

CONCLUSIONS

Side-chain liquid-crystalline polyacrylates **1a–h** containing prochiral sulfide groups present a complex smectic polymorphism including smectic A, B and C mesophases with monolayer and interdigitated bilayer structures. In particular, the lower homologues **1a–f** ($n \leqslant 6$) display smectic B1 and smectic A1 mesophases, whereas the higher homologue **1h** ($n = 10$) forms a bilayer interdigitated smectic C mesophase. Polymer **1g**, with an intermediate sulfide segment length ($n = 8$), appears to be unique in that it gives rise to both monolayer and interdigitated bilayer smectic mesophases in a sequence with increasing temperature. These two structures even coexist over a wide temperature range. Therefore, the progressive lengthening of the terminal sulfide substituent forces the mesogens to move apart, turning from a fully interdigitated smectic structure (S_{A1}) into a looser one (S_{Ad}), and eventually to tilt out to form a bilayer structure with a low degree of interdigitation (S_{Cd}). This structural evolution should be favoured by the presence of a sufficiently long (hexamethylene) spacer segment which is able to decouple the mesogens from the polymer backbone[25]. The coexistence at equilibrium of two different mesophases reflects the multicomponent nature of the polymeric material due to molar mass dispersion, and could be accounted for by assuming that in correspondence to critical structural features, polymer samples with the same repeat unit structure but different molar masses can give rise to different mesophases within close temperature ranges[14]. The length of the alkyl substituent on the sulfide group determines the monolayer and bilayer nature of the smectic mesophase structure. In correspondence to a critical length ($n = 8$) of the sulfide substituent in the polymer repeat unit, the effects of the molar mass and its dispersity are important in determining the incidence and stability of either smectic phase. It is possible that, owing to polymer dispersity, certain molar masses can facilitate the formation of the S_{A1} phase, whereas other molar masses can preferentially stabilize the S_{Ad} phase. Such mesophases will coexist in samples with wide molar mass distributions over a given temperature range and will undergo their distinct phase transitions. To assess this hypothesis, we are presently investigating several samples of **1g** with modulated molar masses and molar mass distributions.

As a final remark, we anticipate that the richness of the smectic mesomorphism exhibited by polymers **1a–h** is promising for the attainment of chiral smectic mesophases by means of the asymmetric oxidation of the prochiral sulfide groups, leading to the corresponding polymers containing chiral sulfoxide groups with prevailing chirality.

ACKNOWLEDGEMENT

Financial support from the Ministero dell'Università e della Ricerca Scientifica e Tecnologica of Italy is acknowledged.

REFERENCES

1 Chiellini, E. and Galli, G. in 'Recent Advances in Liquid-crystalline Polymers' (Ed. L. L. Chapoy), Applied Science, London, 1985, p. 15
2 Chiellini, E. and Galli, G. in 'Recent Advances in Mechanistic and Synthetic Aspects of Polymerization' (Eds M. Fontanille and A. Guyot), Reidel, Dordrecht, 1987, p. 425
3 Le Barny, P. and Dubois, J. C. in 'Side Chain Liquid Crystal Polymers' (Ed. C. B. McArdle), Blackie, Glasgow, 1989, p. 130
4 Shibaev, V. P. and Freidzon, Ya. S. in 'Side Chain Liquid Crystal Polymers' (Ed. C. B. McArdle), Blackie, Glasgow, 1989, p. 260
5 Chiellini, E., Galli, G., Cioni, F. and Dossi, E. *Makromol. Chem. Macromol. Symp.* 1993, **69**, 51
6 Angeloni, A. S., Laus, M., Caretti, D., Chiellini, E. and Galli, G. *Makromol. Chem.* 1990, **191**, 2787
7 Chiellini, E., Galli, G., Angeloni, A. S. and Laus, M. *ACS Symp. Ser.* 1990, **435**, 79
8 Angeloni, A. S., Laus, M., Caretti, D., Chiellini, E. and Galli, G. *Chirality* 1991, **3**, 307
9 Davis, F. A., Jenkins Jr, R. H., Awad, S. B., Stringer, O. D., Watson, W. H. and Galloy, J. J. *J. Am. Chem. Soc.* 1982, **104**, 5412

10 Davis, F. A., Billmers, J. M., Gosciniak, D. J., Towson, J. C. and Bach, R. D. *J. Org. Chem.* 1986, **51**, 4240
11 Freidzon, Ya. S., Kharitonov, A. V., Shibaev, V. P. and Plate, N. A. *Eur. Polym. J.* 1985, **21**, 211
12 Yamaguchi, T., Asada, T., Hayashi, H. and Nakamura, N. *Macromolecules* 1989, **22**, 1141
13 Yamaguchi, T. and Asada, T. *Liq. Cryst.* 1991, **10**, 215
14 Galli, G., Chiellini, E., Laus, M., Angeloni, A. S., Francescangeli, O. and Yang, B. *Macromolecules* 1994, **27**, 303
15 Galli, G., Laus, M. and Angeloni, A. S. *Makromol. Chem.* 1986, **187**, 289
16 Tung, L. H. and Moore, J. C. in 'Fractionation of Synthetic Polymers' (Ed. L. H. Tung), Dekker, New York, 1977, p. 604
17 Stevens, H., Rehage, G. and Finkelmann, H. *Macromolecules* 1984, **17**, 851
18 Percec, V., Tomazos, D. and Pugh, C. *Macromolecules* 1989, **22**, 3259
19 Galli, G., Chiellini, E., Laus, M., Caretti, D. and Angeloni, A. S. *Makromol. Chem., Rapid Commun.* 1991, **12**, 43
20 Laus, M., Angeloni, A. S., Galli, G. and Chiellini, E. *Thermochim. Acta* 1993, **227**, 49
21 Tabrizian, M., Bunel, C., Vairon, J. P., Friedrich, C. and Noël, C. *Makromol. Chem.* 1993, **194**, 689
22 Decobert, G., Dubois, J. C., Esselin, S. and Noël, C. *Liq. Cryst.* 1986, **1**, 307
23 Francescangeli, O., Yang, B., Chiellini, E., Galli, G., Angeloni, A. S. and Laus, M. *Liq. Cryst.* 1993, **14**, 981
24 Noël, C. and Navard, P. *Prog. Polym. Sci.* 1991, **16**, 55
25 Wolff, D., Cackovic, H., Krüger, H., Rübner, J. and Springer, J. *Liq. Cryst.* 1993, **14**, 917